Charge Trapping at Chemically Modified Si(111) Surfaces Studied by Optical Second Harmonic Generation

S. A. Mitchell,* T. R. Ward, D. D. M. Wayner, and G. P. Lopinski

Steacie Institute for Molecular Sciences, National Research Council of Canada, 100 Sussex Drive, Ottawa, Ontario, K1A 0R6, Canada

Received: April 30, 2002; In Final Form: July 16, 2002

Covalent chemical modification of Si(111) surfaces by attachment of organic monolayers with terminal *tert*-butylhydrazide groups is described. Second harmonic generation studies of the hydrazide-modified surfaces in air show the presence of an electric field induced second harmonic (EFISH) response, indicative of charge trapping at the surface. Charge trapping is associated with the hydrazide group and is not observed for other organic monolayers or oxidized silicon surfaces. Charging is reversible and can be modulated by variation of the gaseous ambient of the sample, including particularly oxygen and water vapor. An interpretation is given in terms of ionosorption of O_2 as an electron trap, with strong stabilization of the electron affinity level of O_2 in the monolayer by polar hydrazide groups and adsorbed water molecules. There is also an indication that the hydrazide group may become ionized, as an electron donor. From the dependence of EFISH on laser irradiance and the observation of a transient EFISH response, it is suggested that ionosorption of O_2 may occur spontaneously in the dark and, in addition, is transiently enhanced by laser photoexcitation of silicon. By comparison with EFISH and high-resolution electron energy loss measurements on oxidized silicon surfaces, the density of charge trapped at hydrazide-modified surfaces has been estimated.

1. Introduction

Recent studies by several groups have demonstrated wet chemical procedures for covalent attachment of organic monolayers to silicon crystal surfaces.[1] Such monolayers may provide a means of combining organic molecular properties with silicon semiconductor functionality, in a format suitable for chemical/biochemical sensors or hybrid organic/inorganic electronic devices. Of importance for such applications are electrical properties of the chemically modified silicon surfaces. Hydrogen-terminated Si(111) surfaces formed by etching in aqueous fluoride solution have been shown to be remarkably free of electrically active defects[2−4] and have been used as a starting point for organic chemical modification of Si(111) surfaces.[5−8] Several groups have studied the electrical properties of alkyl-terminated silicon surfaces,[9−12] including for example Si(111)−$C_{10}H_{21}$. The nature of the defects at these interfaces is not known. By comparison, trivalent silicon dangling bond defects known as P_b centers are present at oxidized Si(111) surfaces.[13] These defects trap charge and cause band bending at the Si−SiO_2 interface, which is undesirable for electronic device applications.

In this work, we report on unusual charge trapping phenomena associated with a particular type of organic monolayer covalently attached to the Si(111) surface. The monolayer incorporates a hydrazide (−CO−NH−NH−R) species linked to the surface by an alkyl chain, with a variable organic group R at the outer terminus. In laboratory air, the monolayer adsorbs molecular oxygen, which acts as a trap for electrons from silicon. Under certain conditions, the hydrazide species may also become ionized, by trapping positively charged holes from silicon. The extent of charging of acceptor (O_2) and donor (hydrazide) levels is strongly influenced by variation of the gaseous atmosphere of the sample, including particularly the humidity. Charge trapping at the interface is promoted by the hydrazide groups, which form a thin polar region of the monolayer situated close to the silicon surface. The monolayer is envisaged as liquidlike in some respects, and hence, the static dielectric constant of the polar region is large and strongly stabilizing for charge traps.

The occurrence of charge trapping in the hydrazide film is monitored by electric field-induced optical second harmonic generation (EFISH) measured in reflection from the silicon surface. As discussed in detail by Aktsipetrov and co-workers,[14−17] the second harmonic response of a silicon surface may be greatly enhanced by the presence of an electric field in a space charge region near the surface. The electric field breaks the inversion symmetry of the crystal which otherwise prohibits second harmonic generation (SHG) in the electric-dipole approximation. EFISH has previously been used by several groups to study charge trapping at oxidized silicon surfaces.[18−24] In the simplest case, the observed second harmonic signal varies with the square of the charge density at the interface. In this work, we describe the application of EFISH for studies of charge trapping at chemically modified Si(111) surfaces in laboratory air and under various gaseous ambients at atmospheric pressure. EFISH is advantageous in that no electrical contacts to the sample are needed, the technique is applicable to any interface accessible to light, and measurements are readily time-resolved. Disadvantages of this approach include possible perturbations of the sample by photogenerated charge carriers and limited sensitivity to surface charging in the depletion regime of band bending. The latter depends on the dopant concentration of the silicon crystal. In this paper, we report on EFISH studies of chemically modified Si(111) surfaces using both moderately and highly doped n-type silicon samples.

* To whom correspondence should be addressed.

10.1021/jp026046r CCC: $22.00 Published 2002 by the American Chemical Society
Published on Web 08/29/2002

SCHEME 1

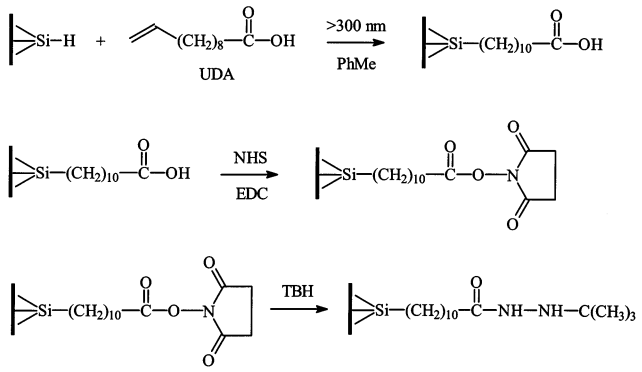

2. Experimental Section

2.1. Preparation of Surfaces. Polished Si(111) wafers were supplied by Virginia Semiconductor, Inc. n-type (1−3 Ω-cm) or n+ (0.0025 Ω-cm) wafers were cut into rhombus-shaped pieces with included angles of 60° and 120° and with side length 17 mm. Chemical modification of the silicon surface followed the sequence shown in Scheme 1.

Hydrogen-terminated Si(111) surfaces were prepared by first sonicating the silicon crystal in Milli-Q water and then cleaning in 1:3 H_2O_2 (30%):H_2SO_4 (conc) at 100 °C for 30 min. The hydrophilic crystal was thoroughly rinsed with milli-Q water and then placed in argon-deaerated ammonium fluoride (40%) for 15 min.[25] The hydrophobic crystal was then dipped in argon-deaerated milli-Q water for several seconds, dried under a stream of inert gas, and immediately utilized for organic derivatization. Undecylenic acid (UDA) modified Si(111) surfaces were prepared by immersing a hydrogen-terminated Si(111) crystal in an argon-deaerated solution of 7% v/v UDA in toluene. The solution was thoroughly purged with argon, sealed in a Pyrex Schlenk tube, and irradiated for 3 h in a Rayonet photochemical reactor (300 nm).[26] The crystal was then rinsed with tetrahydrofuran and dichloromethane (DCM), sonicated for 3 min in DCM, rinsed with DCM, and dried under a stream of inert gas. Derivatized crystals were used immediately for subsequent modification and handled under inert gas. UDA modified Si(111) surfaces were activated with *N*-hydroxysuccinimide (NHS) by immersing the crystal for 1 h in a freshly prepared mixture of a deaerated solution of 1-[3-(dimethylamino)propyl]-3-ethylcarbodiimide hydrochloride (EDC) in water (113 mg/1.5 mL) and a deaerated solution of NHS in water (18 mg/1.5 mL). The mixture was gently purged by bubbling with inert gas. The crystal was then rinsed with water, dried under a stream of inert gas, and used immediately for hydrazide formation. Hydrazide-modified Si(111) surfaces were prepared by immersing a NHS-activated silicon crystal in an argon-deaerated solution of 0.56 mmol *tert*-butylhydrazine hydrochloride (TBH) or cyanophenylhydrazine hydrochloride in 5.0 mL of acetonitrile (ACN) solvent mixture (3.4 mL ACN with 0.8 mL triethylamine and 2-propanol to a total volume of 5.0 mL) for 20 min. The silicon crystal was subsequently rinsed with ACN and dried under a stream of inert gas.

Chemically modified Si(111) surfaces were characterized by FT-IR spectroscopy, X-ray photoelectron spectroscopy (XPS), ellipsometry, and contact angle measurements. For the FT-IR measurements, the Si(111) substrates were attenuated total reflectance (ATR) plates ($25 \times 5 \times 1$ mm^3) supplied by Harrick Scientific Corp. FT-IR spectra were recorded using a Nicolet MAGNA-IR 860 spectrometer at 4 cm^{-1} resolution, using 25 internal reflections at the silicon/ambient interface. The sample compartment was purged with dry nitrogen. XPS measurements were performed using a PHI 5500 system with monochromatic Al Kα_1 photons at 45° incidence and 45° takeoff angle. Samples were transported to the XPS instrument under dry nitrogen and loaded in the analysis chamber within 20 min of their preparation. Film thickness was measured by using a Gaertner model L116 S ellipsometer with a HeNe laser and an angle of incidence of 70°. $n = 1.46$ was used for the film, and $n = 3.85$ and $k = 0.02$ were used for the silicon substrate. Water contact angles were measured by using a Tantek contact angle meter supplied by Cole-Parmer.

2.2. Surface Second Harmonic Generation. The experimental arrangement for optical second harmonic generation (SHG) at chemically modified Si(111) surfaces has been described previously.[27] Laser pulses from a femtosecond optical parametric amplifier (Topas, supplied by Quantronix) were focused on the sample incident at 45° from the surface normal. The reflected second harmonic was isolated by using a Pellin−Broca prism and colored glass filters and detected with a photomultiplier tube and boxcar amplifier. With the pulse energy ~2 μJ, repetition rate 1 kHz, and focal spot diameter ~0.3 mm (measured by translation of a knife edge across the beam waist), the fluence on the sample was ~3 mJ/cm^2 and the average irradiance was ~3 W/cm^2. The pulse duration was ~100 fs. For most measurements, the fundamental wavelength was $\lambda = 714$ nm, which corresponds with a maximum in the SHG response for the Si(111)−H surface.[28]

SHG was studied for samples exposed to laboratory air (22 °C, 25−35% relative humidity) and controlled gaseous ambients at atmospheric pressure. The sample was enclosed in a compact purge box fabricated from Plexiglas with 3 mm diameter holes drilled to pass the incident and reflected laser beams. Dry nitrogen (boil-off from liquid nitrogen reservoir) or dry air (Medical grade from Air Products) were used alone or with a water bubbler to saturate the flowing gas (~3 L/min) with moisture.

In all experiments, a reference SHG signal from a quartz plate was measured simultaneously with the SHG signal from the sample. In addition, all SHG measurements were normalized to a signal that was recorded when a z-cut quartz wedge was substituted in the sample position.[28]

3. Results and Discussion

3.1. Characterization of Chemically Modified Surfaces. For convenience in the discussion, we adopt the following shorthand notation for chemically modified Si(111) surfaces. The crystal type is given as n or n+ as specified in section 2.1, and the chemical state of the surface is abbreviated as OX for native oxide, H for hydrogen-terminated, UDA for modification with undecylenic acid, NHS for NHS-activated surface, TBH for modification with *tert*-butylhydrazide, and CPH for modification with cyanophenylhydrazide. Thus, n/TBH refers to n-type silicon with a *tert*-butylhydrazide monolayer as shown in Scheme 1.

The thickness of freshly prepared films was measured by ellipsometry (Å, relative uncertainty ±1 Å): 12, 16, and 16 for n/UDA, n/NHS, and n/TBH, respectively. These results are consistent with monolayer or submonolayer coverages in all cases. Water contact angles were measured for n/TBH and found to be in the range of 62−65°, which compares with ~100° for decyl-modified Si(111) surfaces.[10] The hydrophobic character of n/TBH is expected to be due to the presence of terminal *tert*-butyl groups, whereas the reduced hydrophobicity relative to the decyl monolayer probably reflects the presence of polar hydrazide groups near the surface.

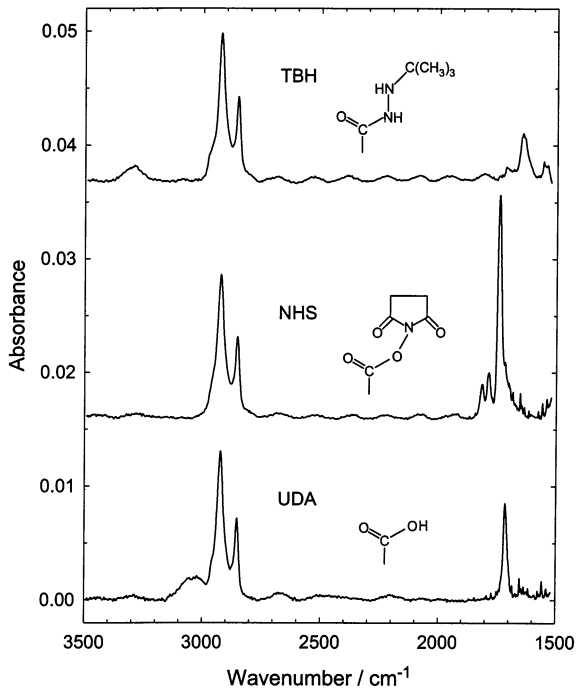

Figure 1. ATR−FTIR spectra of freshly prepared n/UDA, n/NHS, and n/TBH surfaces, offset vertically for clarity. The chemical structures of the terminal groups of the monolayers are illustrated. Wavenumbers of the major peaks are given in Table 1.

TABLE 1: Major Peaks in ATR-FTIR Spectra of Chemically Modified Si(111) Surfaces

monolayer[a]	wavenumbers/cm^{-1}
undecylenic acid (UDA)	3039, 2923, 2853, 1716
N-hydroxysuccinimide-activated (NHS)	2923, 2853, 1815, 1788, 1742
tert-butylhydrazide (TBH)	3292, 2923, 2852, 1645, 1540

[a] Chemical structures of the monolayers are shown in Scheme 1.

Figure 1 shows ATR-FTIR spectra of freshly prepared n/UDA, n/NHS, and n/TBH surfaces, and the wavenumbers of the major peaks are given in Table 1. The optical density in the $\nu(CH_2)$ region near 2900 cm^{-1} is similar in all spectra and similar to that observed previously in this laboratory for decyl-modified Si(111) surfaces.[8] This indicates similar coverages of C_{10}-alkyl chains on all surfaces. The spectra in Figure 1 show characteristic changes with chemical modification, in the carbonyl region near 1700 cm^{-1} and also in the region of ν(OH) ($\sim$3040 cm^{-1}) for n/UDA and ν(NH) ($\sim$3290 cm^{-1}) for n/TBH. These changes are consistent with the surface chemical reactions shown in Scheme 1 and were used to optimize reaction conditions.

The spectrum for n/UDA in Figure 1 is similar to that for liquid decanoic acid,[29] and there is a close correspondence between the spectrum for n/THB and that for liquid *N*-ethylacetamide[29] (for example), which has a similar amide chromophore. Decanoic acid and *N*-ethylacetamide show characteristic shifts between gas-[30] and liquid-phase[29] spectra in the carbonyl and ν(OH) or ν(NH) regions, which reflect intermolecular interactions including hydrogen bonding in condensed phases.[31,32] Table 2 shows comparisons of observed peak positions for n/UDA and n/TBH with data from gas- and liquid-phase spectra for decanoic acid and *N*-ethylacetamide, respectively. It is seen that the spectra of the monolayers are close to those observed for liquids with similar chromophores and significantly different from corresponding gas-phase spectra.

TABLE 2: Peak Positions in ATR-FTIR Spectra of Chemically Modified Si(111) Surfaces Compared with Gas- and Liquid-Phase Spectra of Model Compounds (cm^{-1})[a]

	decanoic acid			*N*-ethylacetamide	
n/UDA	liquid[b]	gas[c]	n/TBH	liquid[b]	gas[c]
3039	$\sim$3000	3576	3292	3291	3470
1716	1711	1778	1645	1655	1717
			1540	1567	1500

[a] Decanoic acid ($CH_3(CH_2)_8COOH$); *N*-ethylacetamide (CH_3CONH-CH_2CH_3). [b] Reference 29. [c] Reference 30.

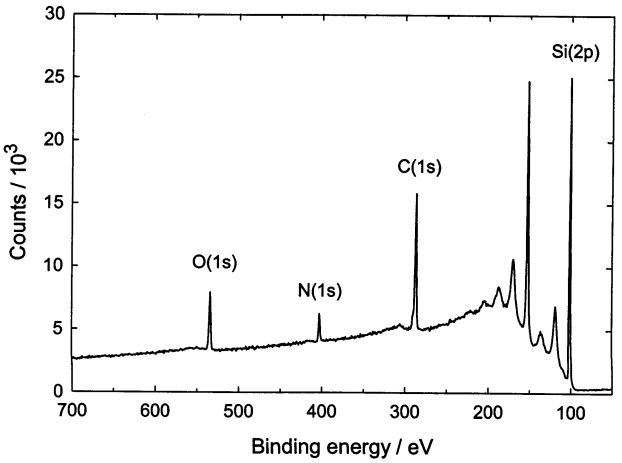

Figure 2. XPS survey spectrum of freshly prepared n/TBH surface, showing core-level features used in analysis of surface coverage.

TABLE 3: Relative Areal Densities and Surface Coverages from Analysis of High Resolution XPS Data for New and Aged N/TBH Surfaces[a]

	[O]/[N][b]	[C]/[N][b]	[C]/[O][b]	Θ(O)[c]	Θ(chains)[c]
n/TBH (new)	1.5	9.5	6.1	1.8	0.26
n/TBH (aged)	1.8	12.1	6.5	2.2	0.34

[a] Details of sample preparation are described in the text. [b] Relative areal densities of atoms from peak areas, using sensitivity factors given in the text. [c] Monolayer coverage of oxygen atoms or hydrazide ($C_{15}H_{31}N_2O$) chains, calculated using the analysis of ref 33. One monolayer corresponds with 7.8×10^{14} cm^{-2}.

This indicates that the carboxylic acid or hydrazide groups in the monolayers experience intermolecular interactions similar to those present in liquids. In particular, the results indicate that hydrogen bonding interactions are important in the monolayer films.

The stability of n/TBH films in laboratory air was investigated by ATR-FTIR spectroscopy. The measurements indicated that the monolayer was stable in air for at least several days. After prolonged storage in air for six weeks, it appeared that the hydrazide had partially decomposed, as shown by loss of characteristic amide features in the carbonyl region and growth of a feature at $\sim$1716 cm^{-1} associated with carboxylic acid (Table 1). This indicates that oxidative decomposition of the hydrazide film occurred in air over a period of several weeks.

An XPS survey spectrum of a freshly prepared n/TBH surface is shown in Figure 2, and the results of an atomic concentration analysis from high resolution scans of O(1s), C(1s), N(1s), and Si(2p) lines are given in Table 3. Results are included for two n/TBH samples: the freshly prepared surface for which the survey spectrum is shown in Figure 2 and a second sample that had been periodically exposed to laboratory air (total exposure $\sim$2 h) but otherwise stored in a dry nitrogen purge for a period of 3 weeks. The second sample was typical of ones that showed

enhanced SHG response as described in section 3.3 below. We shall refer to such samples as "aged" samples. The relative areal densities [O]/[N], [C]/[N], and [C]/[O] in Table 3 were obtained by scaling the XPS intensity data with appropriate sensitivity factors, including instrumental corrections as specified in the PHI analysis software but not including corrections for attenuation of photoelectrons within the monolayer. The relative sensitivity factors were C(1s), 0.314; N(1s), 0.499; O(1s), 0.733; and Si(2p), 0.368. The absolute coverages of O atoms and TBH monolayer chains given in Table 3 were obtained by using the analysis of Cicero et al.,[33] including mean free path parameters for the monolayer and silicon substrate as used by Cicero et al. and atomic sensitivities as given above. The film thickness used in the analysis was 16 Å, as measured by ellipsometry in this work.

From the stoichiometry of the TBH species bonded to the surface, $C_{15}H_{31}N_2O$ (Scheme 1), one expects relative areal densities [O]/[N] ~ 0.5, [C]/[N] ~ 7.5, and [C]/[O] ~ 15. The XPS data in Table 3 indicate that oxygen and carbon were present in excess of the stoichiometric amounts (relative to nitrogen), with slightly greater excesses present in the aged sample. We believe that the excess of oxygen is due to partial oxidation of the silicon interface during the preparation of the surface, including particularly during photochemical modification with UDA. The excess of carbon is most likely the result of contamination. The absolute coverages in Table 3 indicate ~2 monolayers of O atoms and between one-quarter and one-third monolayer coverage of TBH species, for both new and aged n/TBH surfaces. The uncertainties in the absolute coverages are estimated as ±50%. Note that the coverage of oxygen includes oxygen in the monolayer and at the silicon interface. The coverage is thus overestimated because the analysis assumes that all oxygen is present at the silicon interface, with photoelectrons subject to attenuation by the full thickness of the monolayer film.[33] However, the data in Table 3 indicate that most of the oxygen is present at the silicon interface, so the correction is well within the estimated uncertainty.

The XPS results show that new and aged n/TBH films differed only slightly in the extent of oxidation of the silicon interface. This is consistent with ellipsometry measurements that showed minor or insignificant changes in film thickness for new and aged samples. The XPS results also show approximately constant coverage of nitrogen, which indicates minimal decomposition of the monolayer film in the aged sample. Considering also the ATR-FTIR results described above, it can be concluded that new and aged films differed only slightly in the composition of the monolayer film and the extent of oxidation of the silicon interface.

3.2. Second Harmonic Reflection from Si(111) Surfaces. The second-order nonlinear optical response of an unreconstructed Si(111) surface shows rotational anisotropy that reflects the 3-fold symmetry of the surface.[34] In the present work, rotational anisotropy of SHG for *p*-polarized fundamental and second harmonic radiation was measured by rotating the sample about the surface normal. The SHG efficiency R_{pp} is defined in terms of irradiances of fundamental and second harmonic radiation as shown in eq 1:

$$R_{pp} = \frac{I_p(2\omega)}{[I_p(\omega)]^2} \tag{1}$$

Rotational anisotropy of R_{pp} is expressed by eq 2, where ϕ is the azimuthal rotation angle (between the plane of incidence and the $[2\bar{1}\bar{1}]$ direction on the Si(111) surface):[34]

$$\begin{aligned} R_{pp} &= |A_{pp} + B_{pp}\cos(3\phi)|^2 \\ &= |A_{pp}|^2 + |B_{pp}|^2\cos^2(3\phi) + \\ &\quad 2|A_{pp}||B_{pp}|\cos(\theta_{pp})\cos(3\phi) \end{aligned} \tag{2}$$

In eq 2, $|A_{pp}|$ and $|B_{pp}|$ are absolute magnitudes of complex-valued isotropic and anisotropic *effective* second-order susceptibilities, and θ_{pp} is their relative phase (in the range 0−180°), as shown in eq 3:

$$\frac{A_{pp}}{B_{pp}} = \frac{|A_{pp}|}{|B_{pp}|}\exp(i\theta_{pp}) \tag{3}$$

The parameters $|A_{pp}|$, $|B_{pp}|$, and θ_{pp} often show characteristic changes with the chemical state of the Si(111) surface.[27,28] The associated nonlinear polarization has contributions from both surface and bulk sources.[34]

3.3. Effect of Ambient Atmosphere on SHG Efficiency. In Figure 3, we show plots of rotational anisotropy of normalized SHG efficiency for n+/OX, n/OX, n/H, and n/UDA surfaces exposed to laboratory air, for a fundamental wavelength λ = 714 nm. The measurements on n/H and n/UDA surfaces were performed within several minutes of their preparation. The acquisition time for a rotational anisotropy measurement was 3.3 min. The data were fit to eq 2, and the results are summarized in Table 4. Repeated measurements on the same samples were highly reproducible. Each type of sample was prepared several times, and the normalized SHG efficiencies were generally reproducible within ±20%. Note that each surface shows a distinctive pattern of rotational anisotropy, and variations up to 200-fold are observed in the normalized SHG efficiency. Results for freshly prepared n/NHS, n/TBH, and n/CPH surfaces were very similar to those for n/UDA shown in Figure 3. Exposure to air was carefully controlled for all samples.

A peculiar effect was noted for the hydrazide-modified surfaces only and not for the other Si(111) surfaces investigated in this study. For n/TBH and n/CPH, it was found that the SHG efficiency tended to increase on continued exposure of the samples to air. This effect became more pronounced when the samples were reinvestigated after being stored in the dark under a dry nitrogen purge. With increasing storage time under nitrogen for periods of several hours to several weeks, n/TBH and n/CPH surfaces showed a pronounced variation in SHG efficiency as measured in laboratory air. Typical results for n/TBH are shown in Figures 4−6. Figure 4 shows rotational anisotropy data for a freshly prepared n/TBH surface in laboratory air and for the same surface under various ambient atmospheres after being stored under nitrogen for 3 days. Following this storage period, the sample showed a reversible variation in SHG efficiency with ambient atmosphere. For each measurement, the sample was exposed to the selected atmosphere in the purge box for at least 20 min. In laboratory air, the SHG efficiency was almost 3-fold larger than for the freshly prepared sample, but under dry nitrogen, the efficiency was reduced almost to the same level as the fresh sample. Under water-saturated nitrogen, the SHG efficiency was intermediate between these levels. These effects were reversible and could be cycled repeatedly.

For longer storage periods under nitrogen, the effect of the ambient atmosphere during the SHG measurement was more pronounced. Figure 5 shows results for a n/TBH sample after storage for one month under dry nitrogen. During this period, the sample was exposed to air and water-saturated nitrogen for brief intervals during SHG measurements. Comparison with

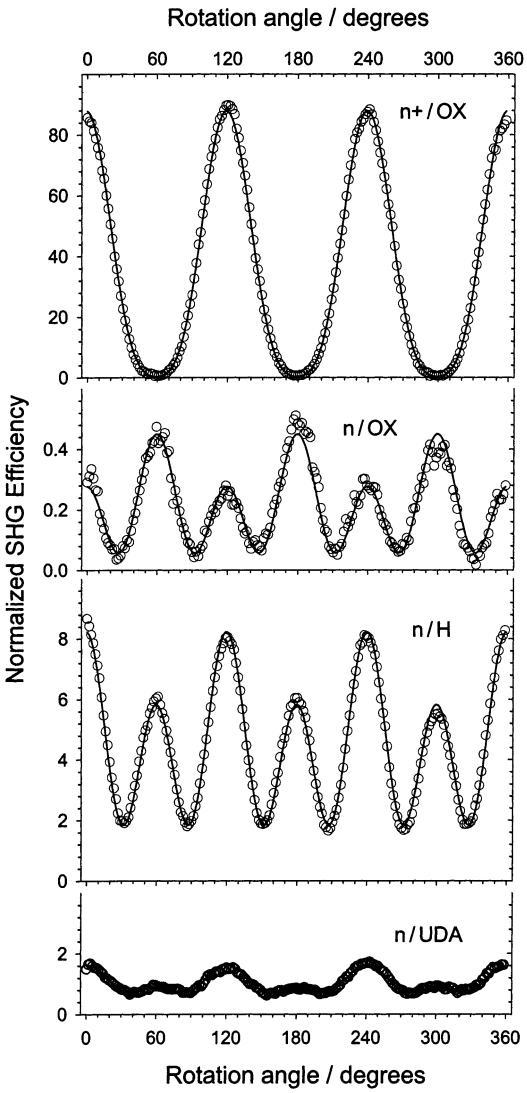

Figure 3. Rotational anisotropy of SHG efficiency R_{pp} for n+/OX, n/OX, n/H, and n/UDA surfaces exposed to laboratory air. The incident laser wavelength was 714 nm. SHG efficiencies have been normalized to the SHG efficiency of z-quartz. Solid lines show fits of the data to eq 2.

TABLE 4: Rotational Anisotropy of Normalized SHG Efficiency for Chemically Modified Si(111) Surfaces, with λ = 714 nm[a]

	Si(111) surface			
parameter	n+/OX	n/OX	n/H	n/UDA
$\lvert A_{pp}\rvert$	5.2	0.30	1.4	0.89
$\lvert B_{pp}\rvert$	3.9	0.48	2.2	0.69
θ_{pp}	0	110	79	73

[a] SHG efficiency normalized to efficiency of z-quartz.

Figure 4 shows that the SHG efficiency in laboratory air was significantly increased following this longer storage period, amounting now to a greater that 6-fold increase compared with the fresh sample. As was the case for the shorter storage period, changing the atmosphere from laboratory air to dry nitrogen resulted in a strong reduction of the SHG efficiency. However, in contrast with the results for the shorter period, the effect of water-saturated nitrogen was to reduce the SHG efficiency further, almost to the level of the fresh sample. Once again these effects were reversible over many cycles.

A further effect was observed for the hydrazide-modified surfaces, involving a time dependent SHG response under

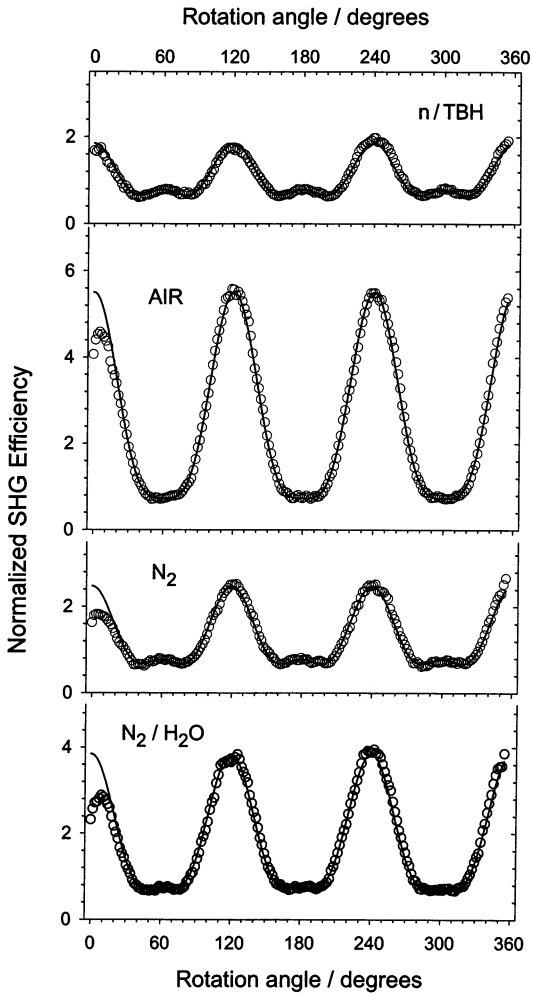

Figure 4. Rotational anisotropy of normalized SHG efficiency R_{pp} for a freshly prepared n/TBH surface in laboratory air (top) and for the same surface exposed to the indicated gaseous ambients after being stored under nitrogen for 3 days. The incident laser wavelength was 714 nm. N_2/H_2O indicates nitrogen saturated with water vapor. The effect of the ambient was reversible and could be cycled repeatedly.

continuous irradiation by the laser beam. Typical results are shown in Figure 6, as measured for the n/TBH samples for which rotational anisotropy results have been shown in Figures 4 and 5. For the sample stored for 3 days, a pronounced transient response was observed, extending for longer that 50 s and varying with the ambient atmosphere. In some cases, this transient SHG response caused a noticeable distortion of the rotational anisotropy plot at small rotation angles (short irradiation times), as seen in Figure 4. The transients shown in Figure 6 were found to be reproducible, although a dark period of at least 10 min (with the laser blocked) was needed to return the sample to the initial state. Similar effects have been observed for oxidized silicon surfaces,[18,20] as discussed in section 3.5. Transient effects were less pronounced for the sample that had been stored for 1 month, as shown in Figure 6B. However, measurements at higher time resolution showed that relatively fast transients were present. We shall return to this point in the discussion below. It should be noted that no indication was found of irreversible changes in the samples caused by the limited laser irradiation that was used for the SHG measurements.

3.4. Electric Field Induced Second Harmonic Generation. The results described above point to electric field induced SHG (EFISH) as a significant effect for the hydrazide-modified

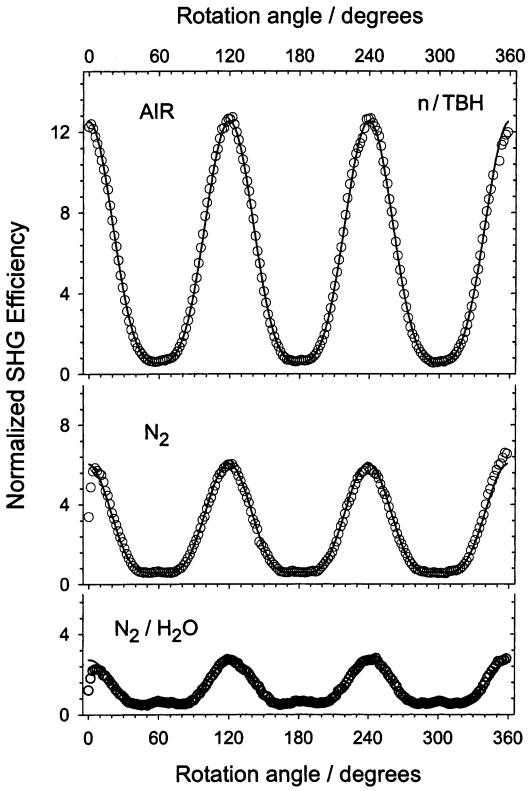

Figure 5. Rotational anisotropy of normalized SHG efficiency R_{pp} for a n/TBH surface exposed to the indicated gaseous ambients after being stored under nitrogen for 1 month. The incident laser wavelength was 714 nm. The effect of the ambient was reversible and could be cycled repeatedly.

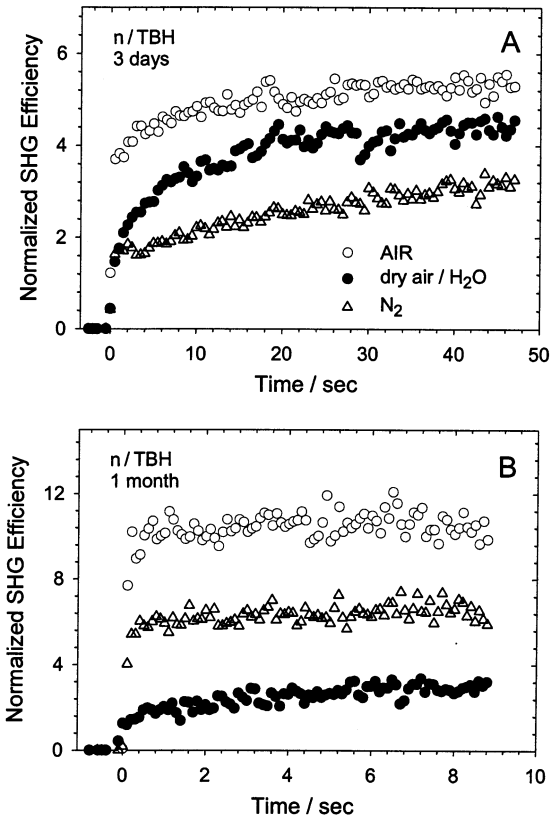

Figure 6. Time dependence of normalized SHG efficiency R_{pp} of n/TBH surfaces under the indicated gaseous ambients following abrupt exposure of surface to laser beam. The legend indicating the ambients applies for A and B. A, sample stored under nitrogen for 3 days; B, sample stored under nitrogen for 1 month. The incident laser wavelength was 714 nm and the azimuthal orientation was set for maximum SHG response at $\phi = 0°$.

surfaces. EFISH is implicated by the correlation of SHG efficiency with exposure of the sample to air, because molecular oxygen can act as an electron acceptor.[18b,35] As discussed below, the occurrence of EFISH is indicative of an accumulation of charge at the interface. The transient SHG response under laser irradiation (Figure 6) is understood as arising from enhanced charge transfer from silicon to interfacial traps (including O_2) induced by photoexcitation of silicon. Also consistent with EFISH is the similarity between the rotational anisotropy patterns observed for n+/OX and n/TBH, specifically in the case of enhanced SHG efficiency for n/TBH (compare Figures 3 and 5). As shown below, the SHG efficiency of n+/OX is unambiguously associated with EFISH, and thus, the rotational anisotropy pattern for n+/OX is characteristic of EFISH. The rotational anisotropy is used here as a diagnostic to indicate a common origin for the nonlinear response for n/TBH and n+/OX. Characteristic features of the EFISH response (for $\lambda =$ 714 nm) include a small or zero value for the relative phase angle θ_{pp}, and a ratio $|A_{pp}|/|B_{pp}| \sim 1.24$, as shown for n+/OX in Table 4. These features are present in the data for n/TBH in air shown in Figure 5 ($\theta_{pp} = 18°$, $|A_{pp}|/|B_{pp}| \sim 1.28$).

To confirm this interpretation the surfaces were studied by second harmonic spectroscopy. In Figure 7, we show the dependence of the anisotropic contribution to the SHG efficiency $|B_{pp}|^2$ on the wavelength of incident laser radiation, for n+/OX, n/H, n/TBH, and n/OX surfaces exposed to air. All SHG measurements were normalized to the SHG efficiency of z-quartz. The various surfaces show characteristic second harmonic spectra, because of resonance-enhancement of SHG at the two-photon level.[36] For comparison, the square of the linear susceptibility of silicon $|\chi^{(1)}|^2$ is also shown in Figure 7, but here, the energy range corresponds with *two* photons on

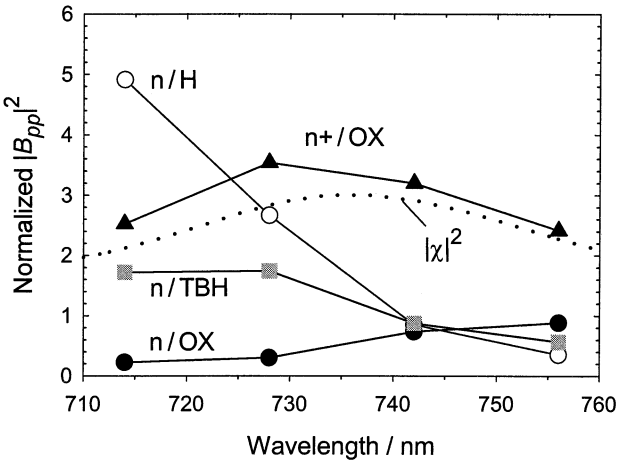

Figure 7. Anisotropic contribution to SHG efficiency $|B_{pp}|^2$ for n+/OX, n/H, n/TBH, and n/OX surfaces as a function of wavelength of incident laser radiation, normalized to SHG efficiency of z-quartz. Data points are connected by straight lines to guide the eye. Relative uncertainties of the points in each spectrum are estimated as ±15%. Measurements for n+/OX have been scaled by a factor 1/6. The broken line shows the square of the linear susceptibility of silicon (in arbitrary units), in the energy range of two photons on the wavelength scale.

the wavelength scale of Figure 7. For EFISH, one expects a close correspondence of the peak maximum of the second harmonic spectrum versus incident photon energy with the maximum of $|\chi^{(1)}|^2$ versus two-photon energy.[37,14] The results in Figure 7 thus confirm the assignment of EFISH as the

dominant contribution for n+/OX. In comparison, EFISH is not important for n/OX, and thus the SHG efficiency is much smaller for n/OX as shown in Figure 3 and Table 4. This is understood from considerations described below. It is also seen in Figure 7 that the second harmonic spectrum of n/TBH is similar to that of n+/OX. This is consistent with the assignment of EFISH for n/TBH exposed to air.

As discussed by Aktsipetrov and co-workers,[15] the intensity of second harmonic radiation due to EFISH at a silicon surface can be expressed as shown in eq 4:

$$I_{pp}^{EFISH}(2\omega) = |C\int_0^{\infty} E(z)\exp(i\Delta z)\,dz|^2 \qquad (4)$$

The subscripts on the left-hand side specify *p*-polarized fundamental and second harmonic radiation. C and Δ are complex-valued constants that depend on the reflection geometry, the linear optical constants of silicon at the fundamental and second harmonic wavelengths, and the third-order nonlinear susceptibility of silicon. $E(z)$ is the spatial distribution of the static electric field in the space-charge region, with z the direction normal to the surface. With knowledge of the dopant concentration in silicon, $E(z)$ can be evaluated from the density of trapped charge at the interface.[15] In certain circumstances, $E(z)$ is effectively constant over the escape depth of second harmonic radiation and can thus be taken outside the integral in eq 4. Then, by Gauss's law, the electric field at the surface is proportional to the interface charge density σ_{int}, so $I_{pp}^{EFISH}(2\omega) \propto |\sigma_{int}|^2$. In the general case, $E(z)$ cannot be considered as constant and this simple relationship does not hold.

In this work, we have used eq 4 to estimate the interfacial charge density associated with the EFISH response observed for n/TBH surfaces. This was done by using a n+/OX surface as a reference for which the magnitude of band bending at the surface was estimated independently. High-resolution electron energy loss spectroscopy (HREELS) has been shown to be a sensitive probe of band bending at semiconductor surfaces through observation of the free carrier plasmon mode.[38] The long-range nature of the dipole scattering mechanism makes it possible to probe substantial distances (~500 Å) into semiconducting and insulating substrates, facilitating observation of band bending effects even in the presence of thin dielectric overlayers. Here, HREELS studies of n+/OX were consistent with a depletion layer thickness ≤20 Å, corresponding to band bending less than 100 meV. We assumed the bands were bent upward (i.e., depletion) by 50 meV and calculated the corresponding EFISH response for n+/OX by using eq 4. Details of the calculations are given in the Appendix. Equation 4 was subsequently used to find the magnitude of band bending for n/TBH such that the calculated EFISH response relative to n+/OX was in agreement with our measurements (ratio ~1/10, see Figures 3 and 5). Our analysis indicates that the interfacial charge density was -2×10^{11} q_e/cm^2 (q_e is the absolute value of the electron charge), and the band bending was 0.7 eV (depletion) for n/TBH surfaces that showed the maximum EFISH response (Figure 5). This corresponds with $\sim 3 \times 10^{-4}$ monolayer of q_e charges at the surface.

These results are reasonable. Band bending near 0.7 eV for n/TBH is in a range where depletion of majority carriers (i.e., electrons) in the space charge region of silicon is strong. Further band bending leads to inversion, where a significant concentration of positively charged holes is present at the surface. From previous studies of moderately doped silicon in the range of the n-type samples used in this work,[16,39] it is known that strong depletion−weak inversion is the range where EFISH becomes the dominant source of second harmonic radiation. For weaker depletion conditions (smaller band bending), the electric field at the surface is much smaller than 10^5 V/cm, and EFISH is relatively weak. Thus, the observation of EFISH as a significant but not dominant contribution to SHG is consistent with band-bending near 0.7 eV. For highly doped samples such as n+/OX, strong electric fields are present even for relatively small band bending. However, to bend the bands of such highly doped samples, it is necessary to trap a relatively high density of charge at the interface. This is the case for n+/OX, where the required high density of interfacial charge is available because of the position of the Fermi energy in the bulk <50 meV from the conduction band edge. In this near-edge region of the band gap, one expects a high density of surface states associated with strained Si−Si bonds at the Si/SiO_2 interface.[13] The relatively small band bending (<100 meV) found for n+/OX from HREELS measurements is expected, because larger band bending would move the band edge away from the Fermi energy and thus the required high density of surface states would not be available. For n/OX, the Fermi energy in the bulk is closer to the middle of the band gap where the density of surface states is relatively small. Interface charging is correspondingly small for n/OX, and EFISH is insignificant. The same applies for n/UDA, n/NHS, and n/H. However, n/TBH shows a different behavior in that charging of the interface depends on the ambient atmosphere of the sample.

3.5. Nature of Charge Traps. Enhancement of EFISH on exposure of n/TBH to air as shown in Figures 4 and 5 is suggestive of electron trapping by molecular oxygen within the monolayer. However, it is also seen in these figures that charge trapping was sensitive to moisture, even when oxygen was excluded from the ambient gas. The effect of the ambient on the charging behavior is complicated, showing a complex pressure dependence that varied with time or "aging" of the sample. There are several indications that more than one type of trap is involved, and below we argue that O_2 acts as a trap for electrons (electron acceptor) and the hydrazide species acts as a trap for positively charges holes (electron donor).

In early investigations of electrical properties of silicon and germanium surfaces, it was found that cycling the ambient atmosphere between, for example, "dry O_2" and "wet N_2" produced large changes in band bending, depending on various surface pretreatment conditions.[40,41] This was interpreted as arising from the effect of the ambient gas on the number density and energy levels of charge traps associated with native oxide films on the surfaces. Trapping of electrons by O_2 molecules at the surfaces of semiconductors is well-known.[35] Recently, EFISH has been used to study charge trapping at oxidized silicon surfaces,[18−24] and "gas assisted" charging of oxide traps by a mechanism involving transiently charged O_2^- surface species has been described.[22] Several studies have focused on time-dependent EFISH effects in which traps at oxidized silicon surfaces are charged by photoinduced processes involving single-photon or multiple-photon excitation of silicon.[18−20] The present work differs from earlier EFISH studies in two significant respects. First, the surfaces studied in this work are not covered with an oxide film. The charging effects studied here are specific to the hydrazide-modified surfaces and were not observed for oxidized silicon surfaces. Second, although photoinduced charging of traps was observed in this work, the EFISH response for aged n/TBH surfaces did *not* show a dominant time-dependent component (Figure 6B). This is in contrast with effects that have been studied for oxidized silicon surfaces, involving pronounced growth of the EFISH signal

during continuous laser irradiation of the sample on the time scale of minutes.[18−20]

It should be noted in this connection that the average irradiance used in the present study (~3 W/cm^2) was much lower than that used in previous work on oxidized silicon surfaces (>10^3 W/cm^2).[18−24] However, the peak power used here was *larger* than in refs 18−24, because of our significantly larger pulse energy (~2 μJ compared with ~10 nJ) at similar pulse duration (~100 fs). The difference in average irradiance is due to the much lower pulse repetition rate used in our work (1 kHz compared with ~100 MHz). van Driel and co-workers[18] have shown that three-photon processes are important in time-dependent EFISH effects observed for oxidized silicon surfaces (with the fundamental wavelength near 800 nm). Such three-photon processes are favored at high peak power, and thus, it is difficult to reconcile the absence of a significant time-dependent EFISH response for n/OX surfaces in our work with the observation of such effects in refs 18−24. One possible explanation is in terms of a photoinduced defect formation process that occurs with significant yield only for large integrated fluence and is thus sensitive to average irradiance. A process of this type has been observed by Cernusca et al.[20] Such defects could facilitate charge trapping by ambient O_2 or they could act as charge traps themselves. Further work is needed to clarify the comparison with previous work on oxidized silicon surfaces.

An important question for the hydrazide-modified surfaces is whether the charging process is photoinduced by the laser or occurs spontaneously in the dark. The time dependence of the EFISH signal following abrupt exposure of the sample to the laser beam provides some indication. Of course, the laser is needed to observe the signal so such a measurement cannot rule out a photoinduced charging process. However, the results for the aged n/TBH sample shown in Figure 6B indicate that, to account for the difference in the prompt EFISH signals for the various ambients, a photoinduced charging process would have to be substantially complete within ~0.5 s. Measurements at higher time resolution reduced this limiting charging time to ~20 ms, corresponding to 20 laser pulses. This is much faster than the observed time dependence of the EFISH signals shown in Figure 6. If the latter are taken as characteristic of relevant photoinduced charging processes, then the limiting rate seems too high and argues against photoinduced charging as the dominant process. A further indication was obtained by observing the time dependent EFISH signal as a function of laser irradiance. If the signal originates from a cascaded process involving photoexcitation of electron−hole pairs in silicon followed by charging of traps and finally EFISH, then a greater than quadratic dependence on irradiance is expected.[18,20,23] This expectation was confirmed in cases where it was obvious that photoinduced charging was important (see for example Figure 6A). However, a nearly quadratic dependence on irradiance was observed for the prompt part of the signal. These results indicate that charge trapping in the hydrazide films occurred by a spontaneous or thermal process, and further charging was induced by laser photoexcitation of the surface.

We propose the following model to explain the main features of our results. The affinity level of O_2 is considered to be strongly stabilized in the hydrazide monolayer, and thus, spontaneous electron transfer occurs from silicon leading to ionosorption of O_2. The trapping sites for O_2^- are sufficiently close to the silicon surface (~10 Å) that electron transfer can occur by tunneling. Charging of the monolayer is reversible, and detrapping occurs at reduced pressure of O_2. Stabilization of O_2^- in the monolayer is attributable to the presence of hydrazide groups, which form a polar layer near the surface with static dielectric properties similar to a liquid. The polar layer has a high affinity for water, so adsorbed water molecules may provide additional stabilization for ions. The structural arrangement of hydrazide groups in the monolayer exerts a strong influence on the energetics of ionosorption, whereas the reversible nature of ionosorption reflects a small net stabilization of O_2^-. The aging process of the monolayer is attributed to a structural relaxation within the monolayer film that favors ionosorption of O_2. Under conditions of high humidity and with significant ionosorption of O_2, the hydrazide species (Hz) may act as an electron donor (i.e., a trap for positive holes from silicon). The donor levels become energetically accessible because of the combined effects of solvation of hydrazide ions (Hz^+) by water and stabilization of Hz^+ by the electrostatic potential of adsorbed O_2^-. The activity of Hz donor levels is suggested by the effect of humidity on the charging behavior of aged n/TBH films, as shown by the EFISH results in Figures 5 and 6B. The effect is striking and indicates a decrease in surface charge density at higher humidity. Our suggestion is that this could come about by ionization of Hz donors. The introduction of positive trapped charge would lead to a decrease in the net negative surface charge density associated with ionosorption of O_2. The result is a decrease in the EFISH response, as seen in Figures 5 and 6B.

Many details of the above model are unspecified, but the main points seem reasonable and well supported by experimental results. A key point concerns the polar nature of the hydrazide layer, which behaves to some extent like a liquid with a high static dielectric constant. The electronic structure of hydrazides of the type R−CO−NH−NH−R′ (where R and R′ are organic substituents) is similar to that of amides (R−CO−NH−R′), as shown by similarities in molecular structures, vibrational spectra, and certain physical and chemical properties.[42,43] Amides are highly polar, and the static dielectric constants of liquid amides are among the highest known.[44] Hydrazides are less well characterized, but the polar nature and hydrogen bonding properties of the amide-like hydrazide group are well established.[42,43] In section 3.1, it was described how the vibrational spectrum of n/TBH is suggestive of a liquidlike structure with hydrogen bonding between hydrazide groups. This gives additional support to the suggestion that the hydrazide groups provide a strongly stabilizing environment for ions, particularly in the presence of humidity. It might be argued that similar behavior should be expected for monolayers of undecylenic acid (UDA), but these films were found not to be active with respect to charge trapping. A rationalization may be found in the reduced polarity and dielectric constants of carboxylic acids relative to amides.[44]

By comparing energy levels including electron affinities for silicon and O_2, it can be estimated that substantial stabilization of O_2^- near 4 eV is required for spontaneous electron transfer from silicon to O_2.[45] We suggest that such a large stabilization may occur by solvation of O_2^- ions by hydrazide species and water molecules in the monolayer. A solvation energy near 4 eV seems reasonable in comparison with established experimental values for solvation of O_2^- by only 1−3 water molecules in the gas phase: 0.85, 1.55, and 2.2 eV for solvation by 1, 2, and 3 water molecules, respectively.[46,47] Recent theoretical studies have predicted a solvation energy of 3.1 eV for O_2^- with a total of five water molecules.[48] As a further indication, the standard reduction potential for O_2 in water (forming solvated O_2^-) is −0.33 V vs normal hydrogen electrode.[49] This

energy level is close to the Fermi energy of the n-type silicon used in this work, and thus electron transfer to O_2 should be feasible in liquid water.[25]

Solvation effects could also induce ionization of hydrazide groups in the monolayer. To our knowledge, the ionization potentials (IP) of isolated hydrazide molecules are not known. For comparison, the IP for 1,1-dimethylhydrazine is 7.3 eV, and that for *N*-ethylacetamide is 8.7 eV.[50] It seems likely that the IP of a *tert*-butylhydrazide would be between these values, which would place it considerably lower than IPs of the other monolayer species studied in this work (e.g., IP of carboxylic acid expected to be ~10 eV).[50] A relatively low IP is expected for hydrazide species because of the presence of the nitrogen (N_α) adjacent to the amide group (i.e., R−CO−NH−N_αH−R). Solvation in the hydrazide monolayer should greatly reduce the ionization potential, and thus, the hydrazide could act as an electron donor or a trap for positively charged holes from silicon. This is a highly speculative but plausible interpretation of the striking effect of humidity in Figures 5 and 6B. In this interpretation, a humid atmosphere leads to a decrease in the net negative surface charge density associated with adsorbed O_2^-, by promoting ionization of Hz donor levels through solvation of Hz^+ ions by adsorbed water molecules.

In the model described above, we have suggested that the aging process of the monolayer may be caused by a structural relaxation within the monolayer film, which produces conditions more favorable for ionosorption of O_2. This suggestion is based on our observations indicating only minor changes in composition of the monolayer and degree of oxidation of the interface during the aging process (section 3.1). We have no evidence to indicate the nature of the assumed structural change. It could involve relaxation of the packing arrangement of the hydrazide groups from an initial, metastable state produced by covalent attachment. Such a structural relaxation could be slow, on the order of days or weeks, considering the importance of dipole−dipole and hydrogen-bonding interactions between the hydrazide groups. The incorporation of solvent molecules in the initial film and their subsequent loss by evaporation could also contribute to a structural instability. An alternative possibility that can be considered to account for the aging process involves the formation of defect states at the interface with silicon. The defects could act as charge traps or they could mediate charge trapping by O_2. Further work is needed to clarify the detailed mechanisms of charge trapping at chemically modified silicon surfaces.

4. Conclusion

In this work, we have described charge trapping phenomena associated with organic monolayers covalently attached to Si(111) surfaces, studied by EFISH. The preparation and characterization of monolayers that incorporate *tert*-butylhydrazide groups has been described. Limited oxidation of the silicon surface accompanies monolayer formation, and the monolayers are stable with respect to oxidation in air for at least several days, as shown by XPS and FT-IR studies. FT-IR spectra show hydrogen bonding interactions between hydrazide groups in the monolayer, similar to liquid- or solid-phase spectra of related hydrazides and amides. On exposure of the hydrazide-modified surface to laboratory air, charge trapping occurs within the monolayer film. The charging is reversible in a nitrogen purge and can be cycled repeatedly. No such charging is observed for silicon surfaces with native oxide films, or with organic monolayers that exclude the hydrazide group. The activity of the surface with respect to charging in air increases over time when the samples are stored in a dry-nitrogen purge for periods of several weeks. Charging of the monolayer in air is thought to occur by spontaneous (i.e., thermally induced) ionosorption of O_2, whereas additional, transient trapping of electrons by O_2 is induced by laser photoexcitation during EFISH measurements. Spontaneous ionosorption is promoted by strong stabilization of adsorbed O_2^- by solvation in the monolayer by polar hydrazide groups and adsorbed water molecules. From the dependence of charging on the ambient atmosphere of the sample, including particularly the humidity, it is suggested that hydrazide groups may also become ionized. The hydrazide groups act as electron donors and, thus, offset the effect of ionosorption of O_2 as an electron acceptor. By comparison with EFISH and HREELS measurements on oxidized silicon surfaces, it was estimated that charging of the hydrazide-modified surface due to ionosorption of O_2 amounted to $\sim 3 \times 10^{-4}$ monolayer of electronic charges.

Appendix

The detailed form of eq 4 in section 3.4 has been given by Aktsipetrov and co-workers.[15] The distribution of the electric field $E(z)$ in the space charge region was derived by numerical integration of Poisson's equation.[51] Separate calculations were performed using Boltzmann and Fermi−Dirac statistics to describe the distributions of free carriers. Neglecting surface quantization effects, $E(z)$ is determined by the magnitude of band bending at the surface and the dopant concentration of silicon. The interfacial charge density is obtained by application of Gauss's law, which relates the field at the surface $E(0)$ to the surface charge density. Equation 4 was used to calculate the variation of $I_{pp}^{EFISH}(2\omega)$ with surface band bending for n and n+ silicon samples (as specified in section 2.1). The dopant concentration was estimated from the resistivity by using data in Sze.[52] For band bending of 0.05 eV (depletion) and n+ silicon, the electric field at the surface was 4.2×10^5 V/cm and the interfacial charge density was -2.7×10^{12} q_e/cm^2 (q_e is the absolute value of the electron charge). Similarly, for band bending of 0.7 eV (depletion) and n silicon, the electric field at the surface was 2.4×10^4 V/cm and the interfacial charge density was -1.6×10^{11} q_e/cm^2. For these values of band bending, the magnitude of $I_{pp}^{EFISH}(2\omega)$ calculated by using eq 4 was greater by a factor of 12 for n+ compared with n silicon. These results were obtained by using Fermi−Dirac statistics. Calculations using Boltzmann statistics gave a charge density higher than noted above for n+ (~20% higher) but closely similar results for n silicon. For n+ silicon, the space charge region was thin (<5 nm) compared with the escape depth of second harmonic radiation (~9 nm), so the assumption of constant $E(z)$ in eq 4 is invalid in this case. For n silicon, however, this assumption was seen to be reasonable.

Supporting Information Available: Graphs of electric field $E(z)$ and potential (band bending) for the calculations described in the Appendix. In addition, tabulations are given of interfacial charge density and second harmonic intensity $I_{pp}^{EFISH}(2\omega)$ calculated for a range of band bending for n and n+ silicon samples. This material is available free of charge via the Internet at http://pubs.acs.org.

References and Notes

(1) For a recent review, see: Buriak, J. M. *Chem. Rev.* **2002**, *102*, 1271.

(2) Yablonovitch, E.; Allara, D. L.; Chang, C. C.; Gmitter, T.; Bright, T. B. *Phys. Rev. Lett.* **1986**, *57*, 249.
(3) Hsu, J. W. P.; Bahr, C. C.; vom Felde, A.; Downey, S. W.; Higashi, G. S.; Cardillo, M. J. *J. Appl. Phys.* **1992**, *71*, 4983.
(4) Angermann, H.; Henrion, W.; Rebien, M.; Fischer, D.; Zettler, J.-T.; Röseler, A. *Thin Solid Films* **1998**, *313*−*314*, 552.
(5) Linford, M. R.; Fenter, P.; Eisenberger, P. M.; Chidsey, C. E. D. *J. Am. Chem. Soc.* **1995**, *117*, 3145.
(6) Bansal, A.; Li, X.; Lauermann, I.; Lewis, N. S.; Yi, S. I.; Weinberg, W. H. *J. Am. Chem. Soc.* **1996**, *118*, 7225.
(7) Effenberger, F.; Götz, G.; Bidlingmaier, B.; Wezstein, M. *Angew. Chem. Int. Ed.* **1998**, *37*, 2462.
(8) Boukherroub, R.; Morin, S.; Bensebaa, F.; Wayner, D. D. M. *Langmuir* **1999**, *15*, 3831.
(9) Bansal, A.; Lewis, N. S. *J. Phys. Chem. B* **1998**, *102*, 1067.
(10) Yu, H.-Z.; Morin, S.; Wayner, D. D. M.; Allongue, P.; de Villeneuve, C. H. *J. Phys. Chem. B* **2000**, *104*, 11157.
(11) Barrelet, C. J.; Robinson, D. B.; Cheng, J.; Hunt, T. P.; Quate, C. F.; Chidsey, C. E. D. *Langmuir* **2001**, *17*, 3460.
(12) Kar, S.; Miramond, C.; Vuillaume, D. *Appl. Phys. Lett.* **2001**, *78*, 1288.
(13) Svensson, C. The Si−SiO_2 system. In *Materials Science Monographs*; Balk, P., Ed.; Elsevier: Amsterdam 1988; Vol. 32, Chapter 5.
(14) Aktsipetrov, O. A.; Fedyanin, A. A.; Melnikov, A. V.; Mishina, E. D.; Rubtsov, A. N.; Anderson, M. H.; Wilson, P. T.; ter Beek, M.; Hu, X. F.; Dadap, J. I.; Downer, M. C. *Phys. Rev. B* **1999**, *60*, 8924.
(15) Aktsipetrov, O. A.; Fedyanin, A. A.; Dadap, J. I.; Downer, M. C. *Laser Phys.* **1996**, *6*, 1142.
(16) Aktsipetrov, O. A.; Fedyanin, A. A.; Mishina, E. D.; Rubtsov, A. N.; van Hasselt, C. W.; Devillers, M. A. C.; Rasing, Th. *Phys. Rev. B* **1996**, *54*, 1825.
(17) Aktsipetrov, O. A.; Baranova, I. M.; Evtyukhov, K. N.; Murzina, T. V.; Chernyi, I. V. *Sov. J. Quantum Electron.* **1992**, *22*, 807.
(18) (a) Mihaychuk, J. G.; Bloch, J.; Lui, Y.; van Driel, H. M. *Opt. Lett.* **1995**, *20*, 2063. (b) Bloch, J.; Mihaychuk, J. G.; van Driel, H. M. *Phys. Rev. Lett.* **1996**, *77*, 920.
(19) Meyer, C.; Lüpke, G.; Lü, Z. G.; Gölz, A.; Kurz, H.; Lucovsky, G. *J. Vac. Sci. Technol. B* **1996**, *14*, 3107.
(20) Cernusca, M.; Heer, R.; Reider, G. A. *Appl. Phys. B* **1998**, *66*, 367.
(21) Mihaychuk, J. G.; Shamir, N.; van Driel, H. M. *Phys. Rev. B* **1999**, *59*, 2164.
(22) Shamir, N.; Mihaychuk, J. G.; van Driel, H. M. *J. Appl. Phys.* **2000**, *88*, 896.
(23) Fomenko, V.; Lami, J.-F.; Borguet, E. *Phys. Rev. B* **2001**, *63*, 121316(R).
(24) Fomenko, V.; Hurth, C.; Ye, T.; Borguet, E. *J. Appl. Phys.* **2002**, *91*, 1.
(25) Wade, C. P.; Chidsey, C. E. D. *Appl. Phys. Lett.* **1997**, *71*, 1679.
(26) Boukherroub, R.; Voicu, R.; Wojtyk, J. T. C.; Wayner, D. D. M. Manuscript in preparation.
(27) Mitchell, S. A.; Boukherroub, R.; Anderson, S. *J. Phys. Chem. B* **2000**, *104*, 7668.
(28) Mitchell, S. A.; Mehendale, M.; Villeneuve, D. M.; Boukherroub, R. *Surf. Sci.* **2001**, *488*, 367.
(29) *Integrated Spectral Data Base System for Organic Compounds, IR*; Tanabe, K.; Tamura, T.; National Institute of Advanced Industrial Science and Technology: Tsukuba, Ibaraki, Japan (http://www.aist.go.jp).
(30) IR and Mass Spectra. In *NIST Chemistry WebBook*, NIST Standard Reference Database Number 69; Linstrom, P. J., Mallard, W. G., Eds.; National Institute of Standards and Technology: Gaithersburg, MD, 2001 (http://webbook.nist.gov).
(31) Miyazama, T.; Shimanouchi, T.; Mizushima, S.-I. *J. Chem. Phys.* **1956**, *24*, 408.
(32) Bellamy, L. J. *The Infrared Spectra of Complex Molecules*, 2nd ed.; Chapman and Hall: London, 1980; Vol. 2, Chapter 5.
(33) Cicero, R. L.; Linford, M. R.; Chidsey, C. E. D. *Langmuir* **2000**, *16*, 5688.
(34) Sipe, J. E.; Moss, D. J.; van Driel, H. M. *Phys. Rev. B* **1987**, *35*, 1129.
(35) Morrison, S. R. *The Chemical Physics of Surfaces*, 2nd ed.; Plenum Press: New York, 1990; Chapter 7.
(36) Daum, W.; Krause, H.-J.; Reichel, U.; Ibach, H. *Phys. Rev. Lett.* **1993**, *71*, 1234.
(37) Godefroy, P.; de Jong, W.; van Hasselt, C. W.; Devillers, M. A. C.; Rasing, Th. *Appl. Phys. Lett.* **1996**, *68*, 1981.
(38) (a) Matz, R.; Luth, H. *Phys. Rev. Lett.* **1981**, *46*, 500. (b) Polyakov, V.; Elbe, A.; Schaefer, J. A. *Appl. Phys. A* **1995**, *60*, 567.
(39) Mitchell, S. A.; Janz, S.; Bardwell, J. A. *Chem. Phys. Lett.* **1999**, *310*, 361.
(40) Frankl, D. R. *Electrical Properties of Semiconductor Surfaces*; Pergamon Press: Oxford, U.K., 1967; Chapter 7.
(41) Many, A.; Goldstein, Y.; Grover, N. B. *Semiconductor Surfaces*; North-Holland: Amsterdam, 1965; Chapter 9.
(42) Smith, P. A. S. *The Chemistry of Open-Chain Organic Nitrogen Compounds*; Benjamin: New York, 1966; Vol. II.
(43) Krueger, P. J. in *The Chemistry of the hydrazo, azo and azoxy groups*; Patai, S., Ed.; Wiley: London, 1975; Chapter 7.
(44) Lide, D. R., Ed.; *Handbook of Chemistry and Physics*, 3rd electronic ed.; CRC Press: Boca Raton, FL, 2000.
(45) The ionization potential of silicon is 5.35 eV (Akremi, A.; Lacharme, J.-P.; Sébenne, C. A. *Surf. Sci.* **1998**, *402*−*404*, 746), and the electron affinity of O_2 is 0.45 eV (ref 50). Assuming a common vacuum level, the bulk properties of silicon place the Fermi energy of the n-type silicon used in the present study ∼4 eV below the electron affinity level of O_2.
(46) Arshadi, M.; Kebarle, P. *J. Phys. Chem.* **1970**, *74*, 1483.
(47) Luong, A. K.; Clements, T. G.; Sowa Resat, M.; Continetti, R. E. *J. Chem. Phys.* **2001**, *114*, 3449.
(48) Lee, H. M.; Kim, K. S. *Mol. Phys.* **2002**, *100*, 875.
(49) Sawyer, D. T. *Oxygen Chemistry*; Oxford University Press: New York, 1991.
(50) Lias, S. G.; Liebman, J. F. Ion Energetics Data. In *NIST Chemistry WebBook*, NIST Standard Reference Database Number 69; Linstrom, P. J., Mallard, W. G., Eds.; National Institute of Standards and Technology: Gaithersburg, MD, 2001 (http://webbook.nist.gov).
(51) Mönch, W. *Semiconductor Surfaces and Interfaces*, 2nd ed.; Springer-Verlag: Berlin, 1995.
(52) Sze, S. M. *Physics of Semiconductor Devices*, 2nd ed.; Wiley: New York, 1981.